

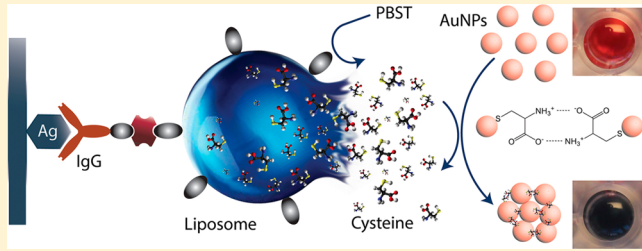
# Single-Digit Pathogen and Attomolar Detection with the Naked Eye Using Liposome-Amplified Plasmonic Immunoassay

Minh-Phuong Bui, Snober Ahmed, and Abdennour Abbas\*

Department of Bioproducts and Biosystems Engineering, University of Minnesota Twin Cities, St. Paul, Minnesota 55108-6005, United States

 Supporting Information

**ABSTRACT:** We introduce an enzyme-free plasmonic immunoassay with a binary (all-or-none) response. The presence of a single pathogen in the sample results in a chemical cascade reaction leading to a large red to dark-blue colorimetric shift visible to the naked eye. The immediate and amplified response is initiated by a triggered breakdown of cysteine-loaded nanoliposomes and subsequent aggregation of plasmonic gold nanoparticles. Our approach enabled visual detection of a single-digit live pathogen of *Salmonella*, *Listeria*, and *E. coli* O157 in water and food samples. Furthermore, the assay allowed a naked-eye detection of target antibody concentrations as low as 6.7 attomolar (600 molecules in 150  $\mu$ L); six orders of magnitude lower than conventional enzyme-linked immunosorbent assay (ELISA).



**KEYWORDS:** Plasmonic colorimetry, immunoassay, signal amplification, liposomes, gold nanoparticles, foodborne pathogens

The ability to detect a single pathogen with the naked eye remains an elusive goal with broad implications in food safety, biodefense, and clinical diagnostics at the early stage of infection. Current technologies rely on sample enrichment via cell culture or nucleic acid-based tests.<sup>1,2</sup> For a large number of diagnostic applications in food safety, biodefense, and healthcare, the primary need is to determine the presence or absence of a pathogen or toxin in the sample regardless of its concentration. When a single *Listeria*, human immunodeficiency virus, anthrax, or ricin molecule is detected, adequate treatment or preventive response will be immediately implemented with no prior need for quantification. When quantification is not the major requirement, then immunoassays can be designed so that they provide a maximum response to any concentration of the target analyte down to a single pathogen, herein referred to as binary or all-or-none response immunoassays.

Various immunoassay solutions have been proposed to overcome the picomolar limit of detection (LOD) of enzyme-linked immunosorbent assay (ELISA).<sup>3,4</sup> Although these assays achieved LOD ranging from the femtomolar ( $10^{-15}$  M) to the attomolar ( $10^{-18}$  M),<sup>5–8</sup> they often require spectroscopic equipment or imaging systems for detection and thus lose the benefit of naked-eye readout offered by ELISA. To enable visual detection of ultralow concentrations with colorimetric assays, a number of strategies have been proposed over the past few years. The best results have been achieved using plasmonic colorimetry, where the color generation is caused by the change in the optical properties (absorbance) of plasmonic nanostructures such as gold or silver nanoparticles.<sup>9</sup> The change in absorbance, i.e., color, of the nanoparticle solution can be

caused by a modification of their size, shape, distribution, or metal composition.<sup>10</sup> In 2011, Qu et al. achieved a LOD of 150 fM ( $10^{-15}$  M) of human immunodeficiency virus by using antibody-conjugated CuO nanoparticles in a sandwich immunoassay and by inducing the aggregation of gold nanoparticles using Cu-catalyzed click chemistry.<sup>11</sup> The next year, the detection limit was further improved beyond the attomolar level ( $10^{-18}$  M) by de la Rica et al., demonstrated by the detection of a viral protein and a cancer biomarker.<sup>12</sup> In their approach, de la Rica et al. used catalase as a biocatalytic enzyme in a conventional ELISA setting to affect the crystal growth of gold nanoparticles (AuNPs), thus inducing a color change in the solution. Although it achieved remarkable detection limits, this method is limited by the chemical instability of hydrogen peroxide in solution and by the dependence on enzyme kinetics, which requires up to 1 h for the generation of the colorimetric signal. Here, we report an enzyme-free colorimetric immunoassay that pushes the LOD with the naked eye to the attomolar level ( $10^{-18}$  M) with instantaneous signal generation and amplification and a clearly defined color shift. The assay demonstrates for the first time a naked eye detection of a single-digit bacteria in food samples, thus overcoming the need for extensive cell culture and plating. This approach builds on our previous work on understanding and controlling AuNP aggregation using molecular cross-linkers<sup>13–15</sup> and on recent advancement in preparing and using loaded liposomes for a variety of applications including drug

**Received:** July 17, 2015

**Revised:** August 8, 2015

**Published:** August 26, 2015



delivery and enzyme catalysis.<sup>16–19</sup> In order to achieve single-digit pathogen detection capabilities with colorimetric tests, we have combined plasmonic colorimetry with a novel molecular signal amplification leading to a liposome-amplified plasmonic immunoassay (LAPIA) shown in Figure 1.

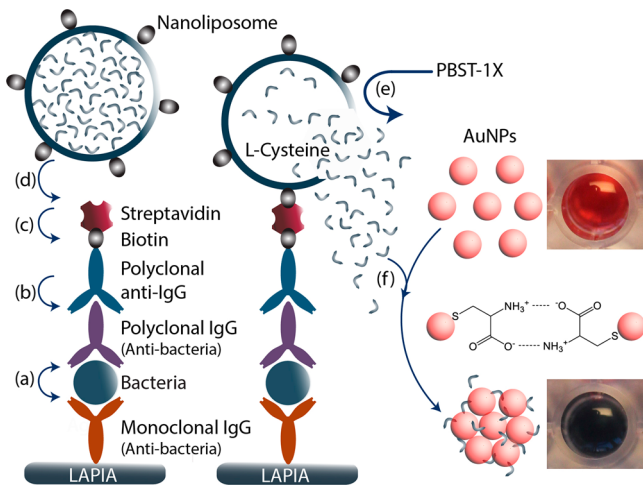


**Figure 1.** Schematic of the liposome-amplified plasmonic immunoassay (LAPIA). One bacterium, molecule, or antigen can rapidly trigger a chemical cascade leading to a chromogenic aggregation of AuNPs. The reaction proceeds in different steps: (a) Capture of the target (biomarker, pathogen, toxin) using sandwich immunoassay. (b) After washing steps, biotinylated secondary antibody (polyclonal anti-IgG) is allowed to interact with the immunocomplex. (c) After incubation and washing, streptavidin is added to interact and bind to biotinylated IgG. (d) After washing steps, biotin-conjugated liposomes containing cysteine are added to the medium followed by AuNP solution. (e) Addition of PBS-Tween-20 1× to the medium causes the breakdown of the liposomes and the release of cysteine, leading to immediate aggregation of gold nanoparticles and color shift from red to dark-blue (f).

Traditionally, immunoassays begin by capturing the target pathogen on a solid surface using specific antibodies in a sandwich immunocomplex format. In ELISA methods, the immunocomplex is conjugated to an enzyme that catalyzes either a chromogenic substrate (conventional ELISA)<sup>3</sup> or a substrate that affects the growth of gold nanoparticles (plasmonic ELISA).<sup>12</sup> In our approach, no enzyme is needed. The immunocomplex is directly labeled with cysteine-loaded liposomes (Cys-liposome) using a biotin–streptavidin linkage. AuNP solution is then added to the assay, followed by the addition of a hydrolytic agent or a buffered surfactant such as PBST (1× PBS buffer with Tween-20 0.05%). In the presence of a pathogen, the surfactant induces immediate hydrolysis of the liposomes, leading to the release of encapsulated cysteine molecules. Due to their high affinity to gold surface, the thiol groups of cysteine will bind to the nanoparticles, while the free amine and carboxyl groups bind to other cysteine molecules via intermolecular hydrogen bonds. The amine groups can also directly interact with the gold surface.<sup>20</sup> By playing the role of a cross-linker, cysteine induces rapid aggregation of AuNPs. Since assembled nanoparticles exhibit light absorbance at higher wavelengths, the aggregation is reflected by a rapid and highly distinctive color shift of the solution from red to dark-blue, which allows naked-eye assessment. The significance of the color shift depends on the degree of nanoparticle aggregation, which in turn depends on the concentration of cysteine cross-

linkers.<sup>13</sup> The main challenge was then to design a reaction system in which the presence of a single pathogen induces maximum aggregation of the nanoparticles. This is achieved by two major features of the LAPIA test: first, the detection mechanism is not limited by enzyme kinetics since no enzyme is used here, and second, each specific antibody is labeled via biotin–streptavidin linkage with one liposome. Each liposome of around 100 nm diameter could contain millions of cysteine molecules. Using liposomes of 400 nm can further increase this number. However, 100 nm liposomes are used here due to their superior stability in solution, minimum fusion, and better encapsulation efficiency.<sup>21,22</sup>

In order to translate this new concept into a working colorimetric assay, we first studied the effect of the different assay components on nanoparticle aggregation and determined the optimum conditions for a stable assay mixture. These conditions ensure that AuNP aggregation (color shift) is only caused by the presence of the target analyte or pathogen and not by any other side reaction or component present in the assay. Since the stability of AuNPs greatly depends on their zeta potential and the pH of the solution, we have prepared mixtures of AuNPs and Cys-liposome at different pH values in order to identify the optimum pH range for LAPIA tests. The synthesized AuNPs solution exhibits a pH of 5.9, and the mixture of AuNPs with Cys-liposome yields a pH of 6.2 with a zeta potential of  $-60\text{ mV}$ . Figure 2a shows that spontaneous aggregation of AuNPs is observed when pH of AuNPs is below 6.5 and quickly reaches maximum aggregation at pH 4.9 where the ionic strength significantly changed the liposome conformation and stability.<sup>23,24</sup> Above pH 6.5, AuNPs remain stable. A control containing the same mixture without cysteine did not yield any aggregation, indicating that low pH caused hydrolysis of the liposomes and the release of cysteine thus causing the aggregation. As a result, we determined the optimum pH of the mixture in LAPIA test to be in the range of 7.0–8.5, which also corresponds to the pH range where cysteine is mostly in a zwitterionic state (see Figure S2 in Supporting Information). Therefore, the pH of the synthesized AuNPs has to be adjusted to the optimum range before use. For instance, when AuNP solution is adjusted to pH 7.25, the assay mixture shows a very high stability, and only the hydrolysis of Cys-liposome by PBST leads to aggregation (Figure 2b). The transmission electron micrographs in Figure 2c,d and Figure S2 in Supporting Information confirm the breakdown of the liposomes by PBST and the subsequent aggregation of AuNPs by cysteine cross-linkers. This aggregation results in the appearance of a second band between 600 and 700 nm in the UV–visible absorption spectra of the nanoparticles, which explains the color shift from red to dark-blue (Figure 2e).

Since the proteins used in a typical immunoassay can also cause aggregation of AuNPs to some extent, we investigated the effect of different concentrations of IgG and BSA, used respectively as a recognition element and a blocking agent. The experiment was performed at pH 7.5 in a mixture containing AuNPs, Cys-liposome, and the protein of interest. Figure 2f shows that BSA has negligible effect on AuNPs stability even at high concentrations, while IgG proteins cause a very low aggregation (<1%) at the usual concentrations used in immunoassays (<5  $\mu\text{g}/\text{mL}$ ).

Once the optimum conditions for the assay stability have been determined, we conducted measurements to evaluate the minimum number of liposomes required to induce maximum

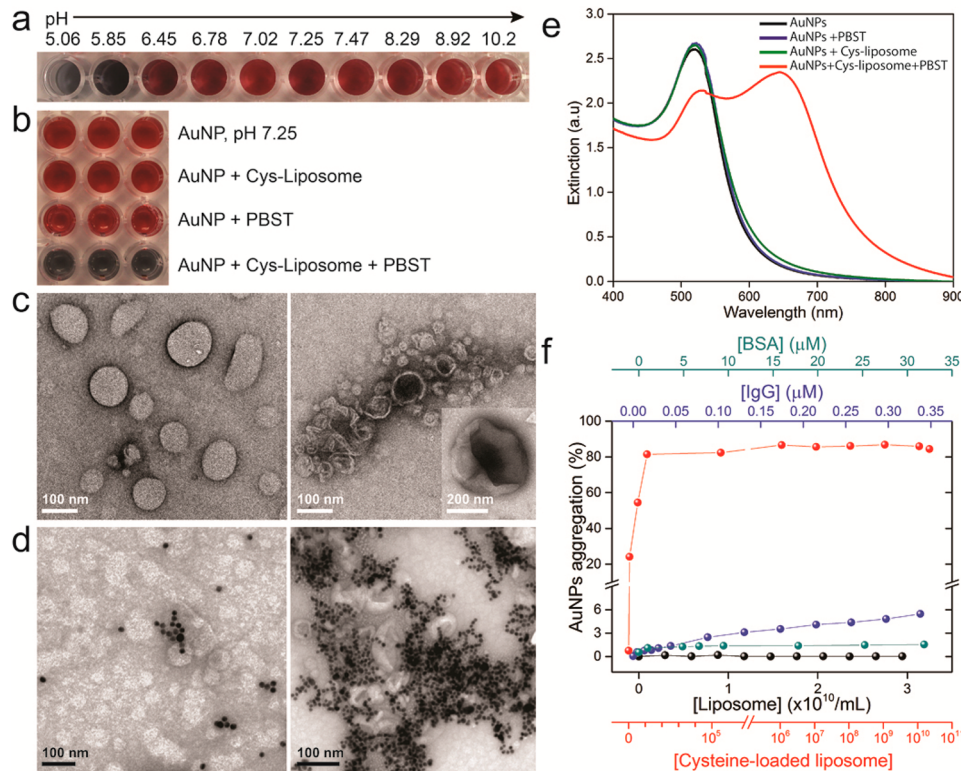


**Figure 2.** Characterization and optimization of the LAPIA test. (a) Optical photograph of AuNP aggregation at different pH values in the presence of cysteine-loaded liposomes (Cys-liposomes) without PBST. The mixture is stable at pH > 6.7. (b) Photograph showing the aggregation of AuNPs upon introduction of PBST 1×. The PBST breaks liposomes and releases cysteine resulting in total aggregation of AuNPs and visible color change from red to dark-blue. The addition of PBST without Cys-liposomes does not cause aggregation. (c) TEM images of intact liposomes (left) and lysed liposomes after exposition to PBST (right). The inset shows a higher magnification image of Cys-liposome after hydrolysis by PBST. (d) TEM images of AuNPs (pH 7.25) in the presence of Cys-liposome solution, before (left) and after (right) adding PBST. (e) UV–vis absorption spectra of single AuNPs in the absence and presence of Cys-liposome and PBST solution (black, blue, green). Single AuNPs are characterized by a single absorption peak at around 520 nm. The addition of PBST caused the appearance of a second band between 600 and 700 nm with a maximum at around 650 nm, characteristic of aggregated or assembled nanoparticles. (f) Effect of BSA, IgG, and nonloaded liposomes on the stability of AuNPs. At concentrations used in typical bioassays, the aggregation is less than 2%. The addition of Cys-liposome and PBST cause total AuNP aggregation (>80%), regardless of the concentration of the liposomes. The number of Cys-liposomes plotted in the graphic is the number needed to cause the aggregation of a 100  $\mu$ L AuNP solution.

nanoparticle aggregation. AuNP solution was mixed with variable concentrations of Cys-liposome and PBST was added to trigger cysteine release, followed by UV–visible absorption spectroscopy and optical density (OD) measurement to estimate AuNP aggregation. The results indicate that around 1000 Cys-liposomes are sufficient to cause a visible aggregation of 25% of 100  $\mu$ L AuNPs, which is still significantly higher than the background signal (<1%) (Figure 2f and Figure S3 in Supporting Information). Although each antigen–antibody immunocomplex can be labeled via biotin–streptavidin linkage with up to three liposomes (streptavidin has four binding sites for biotin), it is unlikely that more than one liposome will bind to the immunocomplex due to steric hindrance. As a result the LOD with the naked eye (nLOD) is expected to be around 17 aM. Such performance also means that single-digit pathogens that would normally bind multiple liposomes through different epitopes would be able to cause significant aggregation and visible colorimetric shift. These predictions will be evaluated through the detection of IgG and three major foodborne pathogens.

To confirm the unprecedented sensitivity of the LAPIA concept and the ability to provide all-or-none response at the attomolar level, rabbit IgG is used as a target analyte in a sandwich immunoassay on a 96-well microtest plate (Figure

3a,b). Cys-liposomes were prepared with biotin-functionalized lipids to enable their binding to biotin-labeled antibodies via streptavidin molecules as described earlier. The schematic of sandwich LAPIA test for the detection of IgG is shown in Figure S4 (Supporting Information). The results show that visible colorimetric shift is obtained for all concentrations down to 6.7 aM, corresponding to around 600 IgG molecules in each microwell of 150  $\mu$ L, which is in agreement with the expected LOD from Figure S3 in Supporting Information. The slight difference between the experimental value (6.7 aM) and the theoretical one (17 aM) is likely due to the difficulties related to evaluating the exact number of liposomes in solution, which is used to calculate the theoretical value.

To optimize the conditions of the IgG detection, the experiment was also performed using different liposome sizes (100 and 200 nm) (Figure 3b). The results reveal similar reactions for the 100 and 200 nm liposomes, with the 100 nm liposomes exhibiting a slightly better performance. Larger liposomes (400 nm) showed fluctuating and less reproducible colorimetric changes. This unexpected result could be explained by the fact that smaller liposomes offer less steric hindrance and more flexibility for liposome interaction with the streptavidin-labeled antibodies. Also, the 400 nm liposomes are likely less stable as revealed by the change in the zeta potential from -36

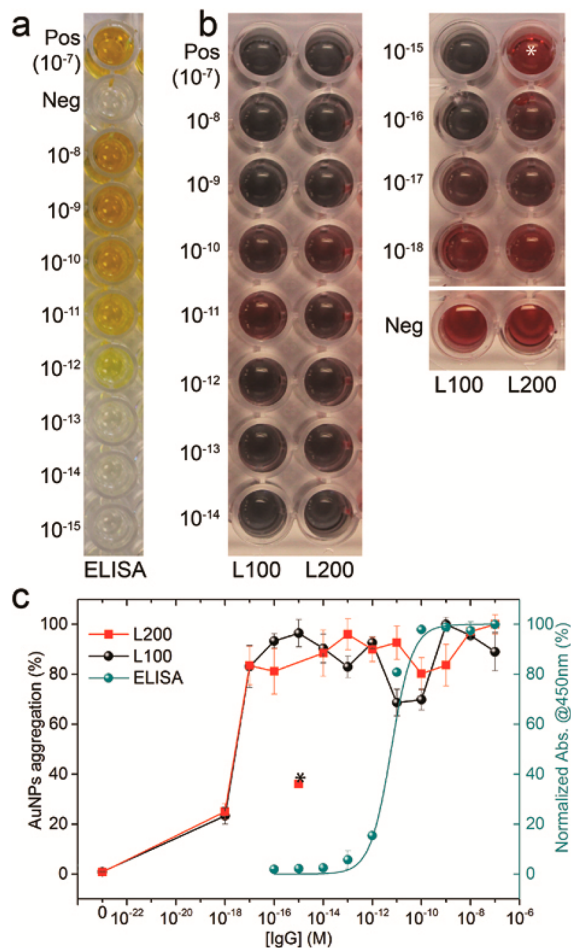


**Figure 3.** Naked-eye detection of rabbit IgG proteins at different concentrations. (a) Conventional ELISA. The yellow color is caused by the biocatalysis of 3',5,5'-tetramethyl-benzidine (TMB) by horseradish peroxidase enzymes. The detection limit is at the picomolar level ( $10^{-12}$  M). (b) LAPIA test. The assay was performed using 100 nm (L100) and 200 nm (L200) liposomes. All tests showed maximum color shift from red to dark-blue at extremely low concentrations down to  $6.7 \times 10^{-17}$  M. A concentration of  $6.7 \times 10^{-18}$  causes 25% aggregation and can still be distinguished from the control. (c) Comparison of the colorimetric response of conventional ELISA and LAPIA tests at different target IgG concentrations. The percentile of AuNP aggregation in LAPIA test is represented with respect to negative control by measuring the optical density at 655 nm. The colorimetric signal of ELISA was recorded at 450 nm. The microwell and corresponding data point indicated with a star represent a false negative. Neg, negative control; Pos, positive control. The concentrations are indicated in molarity (M).

to  $-26$  mV (see Table S1 in Supporting Information). These results also suggest that the cysteine concentration encapsulated in 100 nm liposomes is sufficient to induce significant AuNP aggregation at the attomolar level. Hence, 100 nm liposomes have been used in the following experiments. It is worth noting that the washing steps in these experiments were conducted manually as explained in the methods. It is known that the washing conditions (buffer, pressured wash) can relatively affect the change in color in all ELISA-type assays. This variation can be observed at concentrations of  $10^{-10}$  and  $10^{-11}$  M in Figure 3b, but other experiments showed that this variation could happen at other target concentrations. It is important to note here that even with the variation in color, the

aggregation is always higher than 50%, which is still significantly higher than any false positive we observed so far (<40%), as shown in Figure 3C. The demonstration of live pathogen detection with the LAPIA test was performed on three of the most common pathogenic foodborne bacteria, namely, *Escherichia coli* O157:H7, *Salmonella typhimurium*, and *Listeria monocytogenes*. The microbial suspensions were diluted to different concentrations down to single-digit bacteria (Figure 4a,b). As expected, all bacterial concentrations yielded a maximum colorimetric shift demonstrating a binary or all-or-none response. For ultralow concentrations of  $3 \pm 1$  bacteria per mL, the whole volume of 3 mL from the final dilution is used for cell plating (1 mL) and for the LAPIA test (2 mL). Each 1 mL sample was diluted in 1% PBS-BSA buffer and distributed on eight microwells of 250  $\mu$ L each. Figure 4b reveals that only one to three microwells showed maximum colorimetric shift, with each well containing one to two bacteria, in agreement with the number of bacteria found in the corresponding cell culture plate. This experiment demonstrates the naked eye detection of single-digit pathogens in all-or-none response mode. The visible aggregation of AuNPs in the presence of single-digit pathogens is due not only to the fact that each bacterium can bind multiple Cys-liposomes but also to the fact that the accumulation of liposomes in a small volume around the bacterium results in increased local concentration of released cysteine, which causes rapid aggregation of the surrounding AuNPs. This initial and local aggregation induces a change in the zeta potential of the solution leading to more nanoparticle instability and aggregation without the involvement of cysteine molecules. The detection of the foodborne pathogenic bacteria was performed again by preparing three microtest plates. Each plate was functionalized with antibodies specific to one bacterium, and then exposed to a sample containing the two other bacteria. Figure S5 in Supporting Information shows the absence of colorimetric change indicating the high selectivity of the assay and absence of cross-reactivity. To further confirm the detection abilities of the assay in real-world samples, the same pathogens, i.e., *E. coli*, *Salmonella*, and *Listeria*, were respectively detected at different concentrations in milk, ground beef, and apple juice with no prior treatment of the sample as shown in Figure 5.

In conclusion, we have demonstrated a naked-eye detection of a single-digit pathogens using plasmonic colorimetry of gold nanoparticles combined with signal amplification via cysteine-loaded liposomes. The lowest analyte concentration analyzed and detected with a visible color shift is 6.7 attomolar, which is the lowest reported naked eye LOD without using enzymes or visualization equipment. Concentrations higher than 67 attomolar can be detected with a maximum colorimetric shift indicating an all-or-none response. As proposed here, the assay is suitable for analytical and diagnostic purposes where a binary (Yes or No) response is needed regardless of the concentration of the analyte. This includes pathogen detection in food safety, toxin detection in biodefense, or early detection of infectious agents and identification of minute amounts of biomarkers at the primary stage of disease development where the concentrations are at the subfemtomolar ( $<10^{-15}$  M) level.<sup>25,26</sup> LAPIA concept is applicable for any target analyte as long as its recognition element (antibody, aptamer, complementary DNA, receptor) is available. The concept can also be adapted to enable quantification by adjusting the number of liposomes used or their cysteine payload.

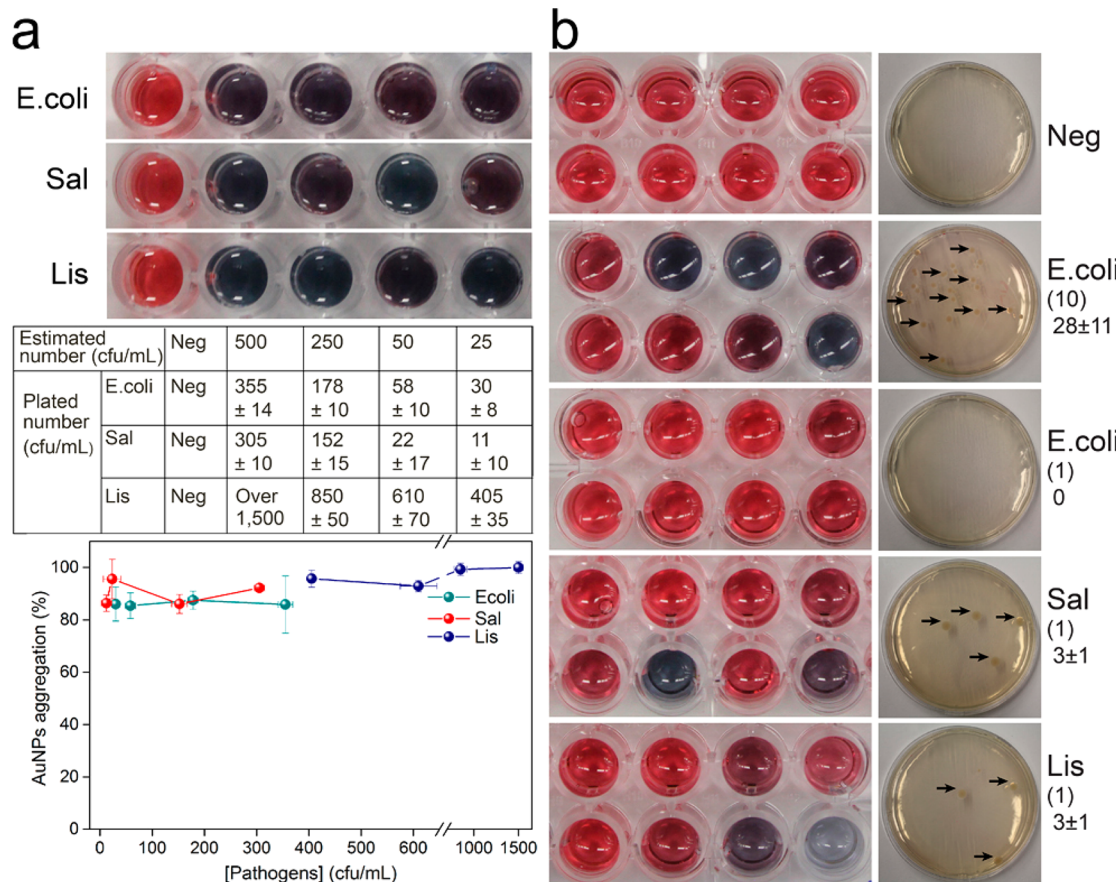


**Figure 4.** (a) Naked-eye detection of foodborne bacteria using LAPIA concept. Optical photographs of LAPIA plates for the detection of *Escherichia coli* O157:H7, *Salmonella typhimurium*, and *Listeria monocytogenes*, labeled respectively E. coli, Sal, and Lis (top). The bacteria were diluted and detected in water at different concentrations. The table represents the estimated and counted number of bacteria using cell plating (middle). The graphic shows all-or-none response for all concentrations with maximum aggregation of AuNPs (absorbance measured at 655 nm) (bottom). (b) LAPIA test detection of foodborne pathogens at single-digit numbers (left), which was confirmed with cell plating (right). At low bacteria numbers (<4 bacteria), only two to three out of eight microwells showed positive response, indicating the detection of one or two bacteria in each well. The estimated (bracketed) and plated bacteria numbers showed consistent results with the LAPIA test.

**Methods. Reagents.** Gold(III) chloride trihydrate, trisodium citrate dehydrate, sodium phosphate saline buffer (PBS), chloroform, bovine serum albumin (BSA), rabbit IgG serum, antirabbit IgG, and streptavidin were purchased from Sigma-Aldrich (USA). L-Cysteine was obtained from Research Products International Corp. (USA). L- $\alpha$ -Phosphatidylcholine and modified phosphoethanolamine were acquired from Avanti Polar Lipids (USA). 20× PBS Tween-20 solution was purchased from Thermo Scientific Inc. (USA) and diluted to 1× concentration containing 10 mM PBS with 0.05% Tween-20 (PBST 1×). Uranyl acetate is obtained from Ted Pella Inc. (USA).

**Preparation of the Bacterial Suspensions.** Three foodborne pathogens, *Escherichia coli* O157:H7 (American Type Culture Collection, (ATCC) 43895), *Salmonella typhimurium* (ATCC14028S), and *Listeria monocytogenes* Scott A (ATCC 19115), were used as sample model, and pathogen manipulation is performed in biosafety laboratory level 2 (BSL-2). The cultures were stored at -80 °C in tryptic soy broth (TSB) (Neogen, USA) with 10% (w/v) glycerol until use. The strains were streaked on tryptic soy agar (TSA) (Neogen, USA) media and incubated overnight. These plates were then used to inoculate TSB broth overnight. The suspensions were adjusted to 0.2 absorbance units at 600 nm using Genesys Visible Spectrophotometer 20 (Thermo Scientific Spectronic, USA).

The suspension was then decimally diluted to different concentrations in physiological saline solution (0.85% NaCl, pH 7.2 ± 0.2). The concentration of different diluted suspensions was confirmed by plating on five TSA plates (200 μL per each) and incubating 24 h before counting the number of colonies.

**Preparation of Cysteine-Loaded Liposomes (Cys-Liposome and Cys-Liposome-Biotin).** L-Cysteine-loaded liposomes were prepared using a reverse-phase evaporation method.<sup>27–29</sup> Briefly, 5 mg of L- $\alpha$ -phosphatidylcholine was dissolved in 1 mL of chloroform solution. The solvent was evaporated to form a thin layer of PC under nitrogen flow and vacuum for 15 min to ensure complete evaporation. The obtained thin film of PC was rehydrated with 5 mL of 50 mM L-cysteine solution in nanopure water to obtain 1 mg/mL final concentration of liposomes. Multilamellar liposomes were formed by whirling until the solution became cloudy and sonicated for 1 min at room temperature. The vesicular solution was then passed through a 100, 200, or 400 nm polycarbonate filter using a mini-extruder (Avanti Inc, USA) to produce homogeneous suspensions of uniform liposome size. Liposome solution was later dialyzed with nanopure water to remove any nonencapsulated cysteine molecules using a dialysis cassette (G2, 3500 MWCO, Thermo Scientific Inc.) for at least

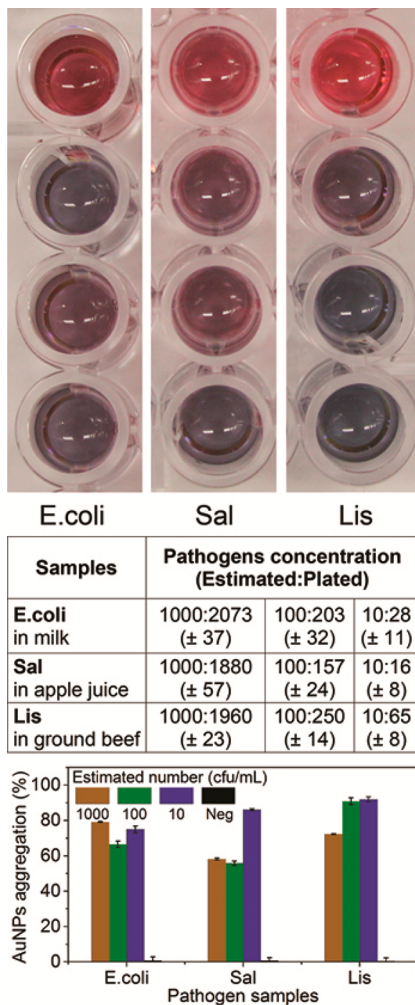


**Figure 5.** LAPIA test for the detection of *E. coli*, *Salmonella*, and *Listeria* in milk, apple juice, and ground beef, respectively. The photograph of the assay showed positive reaction for the three bacteria (top). The number of bacteria in each test was estimated and confirmed with cell plating (middle). The graphic shows the ratio of AuNP aggregation based on absorption measurements at 655 nm (bottom).

1.5 h. The final solution was stored at 4 °C until use. Produced liposomes can be stable for 2–3 weeks at 4 °C.

The preparation of Cys-liposome-biotin was performed using a mixture of L- $\alpha$ -phosphatidylcholine (PC), cholesterol, and phosphoethanolamine-conjugated biotin (PE-PEG2000-biotin) with a molar ratio of 70:10:20, respectively, was dissolved in a chloroform solution (see Figure S6 in *Supporting Information*). The obtained thin film after solvent evaporation was dissolved in cysteine solution as previously described to obtain a final concentration of 1 mg/mL liposome suspension. The rest of the procedure is similar to the one used for the Cys-liposomes. The physical characteristics (size, zeta potential) of the produced liposomes and synthesized gold nanoparticles are determined using dynamic light scattering particle analyzer and Stabino particle charge titration analyzer (from Microtrac, USA). The results are reported in Table S1 in *Supporting Information*.

**Synthesis of Gold Nanoparticles (AuNPs).** All glassware used for AuNPs synthesis was cleaned in Nochromix solution followed by Aqua Regia (3 parts HCl + 1 part HNO<sub>3</sub>)

according to a standard laboratory procedure. The synthesis of citrate-stabilized gold nanoparticles (AuNPs) was based on a modification of Turkevich's method.<sup>30–32</sup> Briefly, a 100 mL solution of 1 mM HAuCl<sub>4</sub> was boiled under stirring and uniform temperature until the formation of bubbles was observed. The solution was then heated for another 25 min. Then, 10 mL of preheated trisodium citrate (38.8 mM) was quickly added to the boiling HAuCl<sub>4</sub> solution. During this process, the solution turns colorless for a moment followed by a transition from violet to dark-ruby/red. The solution was heated for another 5 min before cooling down to room temperature. The final reddish solution of AuNPs was stored at room temperature and covered with aluminum foil. The size of AuNPs was characterized to be 15 ± 2 nm in diameter using transmission electron microscopy (TEM, FEI Technai T12).

**Sandwich LAPIA Test for the Detection of Rabbit IgG.** The experimental schematic for sandwich LAPIA testing was illustrated in Figure S4 (*Supporting Information*). A Sarstedt flat-bottom microtest plate 96-well (Sarstedt Inc., USA) was coated with 150 μL of goat antirabbit IgG (5 μg/mL) in carbonate buffer (pH 9.6) and stored overnight at 4 °C. The plate was then washed three times with washing buffer (1× PBS Tween-20) before exposition to a blocking buffer (5% BSA in 10 mM PBS buffer, pH 7.4) for 2 h at room temperature, followed by washing three times using a washing buffer. After plate coating with antibodies, 150 μL of each diluted polyclonal rabbit IgG solution (from 6.7 × 10<sup>-7</sup> to 6.7 × 10<sup>-18</sup> M) was transferred to the plate according to plate layout and incubated for 1 h at room temperature. After washing three more times, 100 μL of biotinylated polyclonal antirabbit IgG diluted in 1% PBS-BSA buffer solution was transferred to the plate and incubated for 1 h at room temperature. Similar to the previous step, the plate was washed three times followed by the addition of 100 μL of streptavidin solution (1.25 μg/mL) diluted in 1% PBS-BSA buffer at pH 7.4. The plate was incubated for another 30 min at room temperature and then washed twice with washing buffer and twice with 10 mM PBS (pH 7.4) to remove any remaining Tween-20 in the plate. The plate was then incubated for 30 min at room temperature with 50 μL of Cys-liposome-biotin solution diluted in PBS buffer at pH 7.4. After incubation, the plate was gently washed twice by adding 150 μL of PBS buffer (10 mM, pH 7.4) to each well in order to remove the nonbound or weakly bound liposomes.

After washing the plate, 100 μL of AuNP solution at pH 7.25 was added to each well followed by the addition of 15–20 μL of 1× PBST buffer (pH 7.4). Color change from red to dark-blue can be immediately observed in a positive sample. Quantitative analysis of the color shift is realized by reading optical density (OD) values at 655 nm using a microplate reader (iMark, Bio-Rad, USA) and by UV-visible spectroscopy (Shimadzu 1800 spectrophotometer) to evaluate the aggregation degree (%). The aggregation degree is represented by the ratio of the peak area of the absorption band at 650 nm (caused by aggregated AuNPs) and the band at 520 nm caused by single AuNPs. While microplate readers are convenient for conventional ELISA based on enzyme colorimetry and substrate absorbance at a single wavelength, plasmonic colorimetry is more accurately monitored by UV-visible absorption spectrometry. This is due to the fact that the absorption band maximum caused by AuNP aggregation shifts toward higher wavelengths (from 600 nm to around 650 nm) during the aggregation process. This dynamic change of the aggregation

degree can only be recorded by a spectrometer with wavelength scanning.

**Conventional Sandwich ELISA for the Detection of Rabbit IgG.** The procedure for conventional ELISA was performed in a similar manner to LAPIA method with the use of streptavidin conjugated horseradish peroxidase (STV-HRP) enzyme (Thermo Scientific Inc.). The biocatalysis of the substrate, 3,3',5,5'-teramethylbenzidine (TMB) into a colored product was detected using a microplate reader at 450 nm. The color generated by TMB substrate is initially blue and then turns yellow after adding the stop solution.

**Sandwich LAPIA Test for the Detection of Foodborne Pathogens.** Three live pathogens, *Escherichia coli* O157:H7, *Salmonella typhimurium*, and *Listeria monocytogenes*, were used as models for the LAPIA immunoassay. Bacterial suspensions were diluted to different concentrations in physiological saline solution. Polystyrene plates (96-well, Sarstedt Inc., USA) were modified with 100  $\mu$ L of goat antimouse IgG antibodies (Fc specific) and diluted to concentration of 3  $\mu$ g/mL in carbonate buffer (100 mM, pH 9.6). After washing three times with washing buffer, the plates were blocked with blocking buffer (5% BSA in 10 mM PBS buffer, pH 7.4) for 2 h at room temperature. Then, 100  $\mu$ L (2  $\mu$ g/mL) of mouse monoclonal anti-*E. coli* O157:H7, anti-*Salmonella typhimurium*, or anti-*Listeria monocytogenes* (Abcam, USA) was added and incubated for 1 h at room temperature or overnight at 4 °C. After washing again three times, different pathogen suspensions were diluted in 1% PBS-BSA at pH 7.4 with a volume ratio of 1:1, and then added to the plate. After 1 h incubation at 37 °C and washing three times, 100  $\mu$ L of polyclonal anti-*E. coli* O157 (2  $\mu$ g/mL), anti-*Salmonella*, or anti-*Listeria* (4  $\mu$ g/mL), diluted in blocking buffer, was added to the plates and incubated for 1 h at 37 °C. The plates were then washed three times, and 100  $\mu$ L of biotinylated IgG diluted 1:1000 in blocking buffer was added and incubated for 1 h at 37 °C. After another washing cycle, 100  $\mu$ L (2  $\mu$ g/mL) of streptavidin in blocking buffer was added and incubated for another 30 min at room temperature. Then, the plates were washed twice with washing buffer and twice with 10 mM PBS, pH 7.4, to remove any Tween 20 remaining in the plate. The plates were then incubated with 50  $\mu$ L of Cys-liposome-biotin solution (diluted to 1:1 volume ratio in PBS buffer, pH 7.4) for 30 min at room temperature. After a final washing cycle with PBS buffer to remove the nonbound liposomes, colorimetric detection was performed following the same procedure previously described for IgG detection with AuNP aggregation.

**Detection of Foodborne Pathogens in Food Samples.** To study the impact of food matrices on the detection of pathogens using LAPIA test, selected food samples were exposed to known concentrations of a specific foodborne bacterium. Briefly, milk and apple juice were used as purchased and were respectively inoculated with *E. coli* and *Salmonella*. Ground beef (25 g) was mixed in 25 mL of PBS buffer at pH 7.4, and then the suspension was filtered through polycarbonate membrane (0.2  $\mu$ m) and the filtered solution inoculated with *Listeria* before use. All food samples were exposed to known concentrations of pathogens, which were later determined by cell plating in 1% diluted PBS-BSA buffer solution, with a volume ratio of 5:5:2 for bacterial suspension, food matrix, and diluted buffer solution, respectively. The LAPIA test was performed using the same procedure mentioned previously.

## ■ ASSOCIATED CONTENT

### § Supporting Information

The Supporting Information is available free of charge via the Internet at [".](#) The Supporting Information is available free of charge on the ACS Publications website at DOI: [10.1021/acs.nanolett.5b02837](https://doi.org/10.1021/acs.nanolett.5b02837).

Calculation of AuNP aggregation degree and number of liposomes; characterization of liposomes, AuNP, chemical structure, and ionization degree of L-cysteine; schematic of the LAPIA test for rabbit IgG detection; additional TEM and optical images of LAPIA ([PDF](#))

## ■ AUTHOR INFORMATION

### Corresponding Author

\*E-mail: [aabbas@umn.edu](mailto:aabbas@umn.edu). Phone: +1 (612) 624-4292.

### Author Contributions

M.-P.N.B. performed most of the experiments, analyzed the data, and participated in experiment design and scientific discussions. S.A. helped with gold nanoparticle and liposome synthesis and characterization and contributed to result discussions. A.A. proposed the concept, designed the experiments, directed the project, and wrote the paper with input from M.-P.N.B.

### Notes

The authors declare no competing financial interest.

## ■ ACKNOWLEDGMENTS

The authors thank Prof. Jonathan Shilling (University of Minnesota Twin Cities) for providing access to some equipment used in this work. This work is supported by the University of Minnesota MnDRIVE Global Food Venture, and the USDA National Institute of Food and Agriculture, Hatch project 1006789. Parts of this work were carried out in the Characterization Facility, University of Minnesota, which receives partial support from NSF through the MRSEC program.

## ■ REFERENCES

- (1) Cho, I.-H.; Radadia, A. D.; Farokhzad, K.; Ximenes, E.; Bae, E.; Singh, A. K.; Oliver, H.; Ladisch, M.; Bhunia, A.; Applegate, B.; Mauer, L.; Bashir, R.; Irudayaraj, J. *Annu. Rev. Anal. Chem.* **2014**, *7*, 65–88.
- (2) Pollok, S.; Weber, K.; Bauer, M.; Popp, J. *Modern Techniques for Pathogen Detection*; Wiley-VCH Verlag GmbH & Co. KGaA: Berlin, Germany, 2015; p 330.
- (3) Swierczewska, M.; Liu, G.; Lee, S.; Chen, X. *Chem. Soc. Rev.* **2012**, *41*, 2641–2655.
- (4) Lequin, R. M. *Clin. Chem.* **2005**, *51*, 2415–2418.
- (5) Rissin, D. M.; Kan, C. W.; Campbell, T. G.; Howes, S. C.; Fournier, D. R.; Song, L.; Piech, T.; Patel, P. P.; Chang, L.; Rivnak, A. J.; Ferrell, E. P.; Randall, J. D.; Provuncher, G. K.; Walt, D. R.; Duffy, D. C. *Nat. Biotechnol.* **2010**, *28*, 595–599.
- (6) Chen, S.; Svedendahl, M.; Duyne, R. P. V.; Käll, M. *Nano Lett.* **2011**, *11*, 1826–1830.
- (7) de la Rica, R.; Stevens, M. M. *Nat. Protoc.* **2013**, *8*, 1759–1764.
- (8) Kosaka, P. M.; Pini, V.; Ruz, J. J.; da Silva, R. A.; González, M. U.; Ramos, D.; Calleja, M.; Tamayo, J. *Nat. Nano* **2014**, *9*, 1047–1053.
- (9) Anker, J. N.; Hall, W. P.; Lyandres, O.; Shah, N. C.; Zhao, J.; Van Duyne, R. P. *Nat. Mater.* **2008**, *7*, 442–453.
- (10) Willets, K. A.; Van Duyne, R. P. *Annu. Rev. Phys. Chem.* **2007**, *58*, 267–297.
- (11) Qu, W.; Liu, Y.; Liu, D.; Wang, Z.; Jiang, X. *Angew. Chem., Int. Ed.* **2011**, *50*, 3442–3445.
- (12) de la Rica, R.; Stevens, M. M. *Nat. Nanotechnol.* **2012**, *7*, 821–824.

- (13) Abbas, A.; Kattumenu, R.; Tian, L.; Singamaneni, S. *Langmuir* **2013**, *29*, 56–64.
- (14) Gandra, N.; Abbas, A.; Tian, L.; Singamaneni, S. *Nano Lett.* **2012**, *12*, 2645–2651.
- (15) Abbas, A.; Tian, L.; Kattumenu, R.; Halim, A.; Singamaneni, S. *Chem. Commun.* **2012**, *48*, 1677–1679.
- (16) Ngo, A. T.; Karam, P.; Fuller, E.; Burger, M.; Cosa, G. *J. Am. Chem. Soc.* **2008**, *130*, 457–459.
- (17) Aili, D.; Mager, M.; Roche, D.; Stevens, M. M. *Nano Lett.* **2010**, *11*, 1401–1405.
- (18) Tabaei, S. R.; Rabe, M.; Zetterberg, H.; Zhdanov, V. P.; Höök, F. *J. Am. Chem. Soc.* **2013**, *135*, 14151–14158.
- (19) Lichtenberg, D.; Barenholz, Y. Liposomes: Preparation, Characterization, and Preservation. In *Methods of Biochemical Analysis*; John Wiley & Sons, Inc.: New York, 2006; pp 337–462.
- (20) Acres, R. G.; Feyer, V.; Tsud, N.; Carlino, E.; Prince, K. C. *J. Phys. Chem. C* **2014**, *118*, 10481–10487.
- (21) Winterhalter, M.; Lasic, D. D. *Chem. Phys. Lipids* **1993**, *64*, 35–43.
- (22) Sabin, J.; Prieto, G.; Ruso, J. M.; Hidalgo-Álvarez, R.; Sarmiento, F. *Eur. Phys. J. E: Soft Matter Biol. Phys.* **2006**, *20*, 401–408.
- (23) Sulkowski, W. W.; Pentak, D.; Nowak, K.; Sulkowska, A. *J. Mol. Struct.* **2005**, *744–747*, 737–747.
- (24) Yin, M. C.; Faustman, C. *J. Agric. Food Chem.* **1993**, *41*, 853–857.
- (25) Thaxton, C. S.; Elghanian, R.; Thomas, A. D.; Stoeva, S. I.; Lee, J.-S.; Smith, N. D.; Schaeffer, A. J.; Klocker, H.; Horninger, W.; Bartsch, G.; Mirkin, C. A. *Proc. Natl. Acad. Sci. U. S. A.* **2009**, *106*, 18437–18442.
- (26) Etzioni, R.; Urban, N.; Ramsey, S.; McIntosh, M.; Schwartz, S.; Reid, B.; Radich, J.; Anderson, G.; Hartwell, L. *Nat. Rev. Cancer* **2003**, *3*, 243–252.
- (27) Gomes, J. F. P. d. S.; Sonnen, A. F. P.; Kronenberger, A.; Fritz, J.; Coelho, M. Á. N.; Fournier, D.; Fournier-Nöel, C.; Mauzac, M.; Winterhalter, M. *Langmuir* **2006**, *22*, 7755–7759.
- (28) An, S. Y.; Bui, M.-P. N.; Nam, Y. J.; Han, K. N.; Li, C. A.; Choo, J.; Lee, E. K.; Katoh, S.; Kumada, Y.; Seong, G. H. *J. Colloid Interface Sci.* **2009**, *331*, 98–103.
- (29) Roberts, M. A.; Locascio-Brown, L.; MacCrehan, W. A.; Durst, R. A. *Anal. Chem.* **1996**, *68*, 3434–3440.
- (30) Turkevich, J.; Stevenson, P. C.; Hillier, J. *Discuss. Faraday Soc.* **1951**, *11*, 55–75.
- (31) Enustun, B. V.; Turkevich, J. *J. Am. Chem. Soc.* **1963**, *85*, 3317–3328.
- (32) Grabar, K. C.; Freeman, R. G.; Hommer, M. B.; Natan, M. J. *Anal. Chem.* **1995**, *67*, 735–743.